Appl. Phys. B
DOI 10.1007/s00340-013-5554-7

Applied Physics B
Lasers and Optics

Laser ultrasonic receivers based on organic photorefractive polymer composites

Saeid Zamiri · Bernhard Reitinger · Engelbert Portenkirchner · Thomas Berer · Enrique Font-Sanchis · Peter Burgholzer · Niyazi Serdar Sariciftci · Siegfried Bauer · Fernando Fernández-Lázaro

Received: 10 December 2012 / Accepted: 12 June 2013

Abstract We present two laser ultrasonic receivers based on organic photorefractive polymer composites with 2-[4-bis(2-methoxyethyl)aminobenzylidene]malononitrile (AODCST) or 2-dicyanomethylen-3-cyano-5,5-dimethyl-4-(4′-dihexylaminophenyl)-2,5-dihydrofuran nonlinear optical chromophores. Experimental results show sensitivities of the ultrasonic receivers of $\sim 9.5 \times 10^{-8}$ nm $(W/Hz)^{0.5}$ for both composites, and a faster response time ($\sim$60 ms) for the AODCST-based laser ultrasonic receiver. We show that such LUS detectors are highly suitable for contactless thickness measurements of aluminum, steel sheets and defect detection with an accuracy of 100 μm.

S. Zamiri · T. Berer · P. Burgholzer
Christian Doppler Laboratory for Photoacoustic Imaging and Laser Ultrasonic, Science Park 2, Altenberger Straße 69, 4040 Linz, Austria

S. Zamiri (✉) · B. Reitinger · T. Berer · P. Burgholzer
Research Center for Non-Destructive Testing GmbH (RECENDT), Science Park 2, Altenberger Straße 69, 4040 Linz, Austria
e-mail: saeid.zamiri@recendt.at

E. Portenkirchner · N. S. Sariciftci
Linz Institute for Organic Solar Cells (LIOS), Physical Chemistry, Johannes Kepler University, Altenberger Straße 69, 4040 Linz, Austria

E. Font-Sanchis · F. Fernández-Lázaro
División de Química Orgánica, Instituto de Bioingeniería, Universidad Miguel Hernández, 03202 Elche, Spain

S. Bauer
Department of Soft Matter Physics, Johannes Kepler University, Altenberger Straße 69, 4040 Linz, Austria

1 Introduction

Laser ultrasound (LUS) is a remote and contactless measurement technique for materials inspection and characterization [1] in hazardous environments or on small areas. In LUS, a short pulse length laser beam is focused on the sample surface to generate ultrasonic waves, which are remotely detected at the surface of the specimen. Noncontact detection of the ultrasonic waves is achieved by means of interferometers. On samples with rough surfaces, LUS receivers based on two-wave mixing (TWM) in an adaptive photorefractive material (PR) beam combiner exhibit high sensitivity [2].

Besides single-crystal photorefractive materials [2, 3] also polymer composites were used as adaptive beam combiner in PR interferometers [4, 5], with different sensitivities, coupling gains and response times [6]. PR polymer composites are very promising because they have a higher photorefractive coupling gain in comparison with PR crystals. Additionally, PR polymer composites are low cost, they are easily prepared, and they can be tuned for a wide range of wavelengths [6].

In this paper, we report on LUS homodyne detectors based on two different organic PR composites. Both materials are based on a mixture of phenyl-C61-butyric acid methyl ester (PCBM) as sensitizer, poly(*N*-vinylcarbazole) (PVK) as hole transporting polymer, either 2-[4-bis(2-methoxyethyl)aminobenzylidene]malononitrile (AODCST) or 2-dicyanomethylen-3-cyano-5,5-dimethyl-4-(4′-dihexylaminophenyl)-2,5-dihydrofuran (DCDHF-6) as nonlinear optical chromophores (NLOs), and liquid butyl benzyl phthalate (BBP) as plasticizer. We determine and compare the optical coupling gains, sensitivities and response times of the composites and show that polymer-based LUS is highly suitable for the remote measurement of the thickness of metal sheets.

Published online: 07 July 2013

2 Experimental results and discussion

2.1 Sample preparation and characterization

Two types of organic PR composite polymers, DCDHF-6:PVK:BBP:PCBM and AODCST:PVK:BBP:PCBM with ratios of 35:49.5:15:0.5 wt% [6], were used in this work. PVK, PCBM and BBP were obtained from commercial sources, while DCDHF-6 [7] and AODCST [8] (Fig. 1a, b) were synthesized as reported in the literature. The composites were prepared by stirring the constituents in chlorobenzene overnight. Two glass substrates with indium–tin–oxide (ITO) coatings were used to place the PR polymers in between. For fabrication of the conducting electrodes, an area of 1×2 cm^2on each substrate was covered with scotch tape and put in a bath of hydrochloric acid to etch the ITO from the unprotected region to shape the electrodes. The polymer mixtures were dripped on the first etched ITO glass substrates at 45 °C and were dried over night in an oven at 100 °C. Small amounts of each composite were cut and melted on the substrates at 130 °C; 100-μm-thick glass spacers were placed around the composite to homogenize the film thickness. Then, the second etched ITO glass plates were pressed on top of the film (Fig. 1c).

Figure 2 shows the absorption coefficient of the films in the wavelength range between 500 and 800 nm. The inset in Fig. 2 shows the normalized absorption of the polymer composites in solution with absorption peaks at 497 and 434 nm for DCDHF6 and AODCST, respectively. The spectra were acquired using UV–Visible spectrometer (Varian Cary-3G). At a wavelength of 633 nm, the samples exhibit low absorption coefficients α of about 18.7 and 12.8 cm^{-1} for DCDHF6 and AODCST, respectively. The higher absorption coefficient of DCDHF6 in comparison with AODCST is also expected from the normalized absorption peaks shown in the inset of Fig. 2. The refractive indices of the polymer composites were measured to be $n = 1.55$ by using transmission ellipsometry.

2.2 LUS experimental setup

Figure 3 shows the experimental setup of the LUS receiver. A 4-mW He–Ne laser with a wavelength of 632.8 nm was used as detection laser. An external high voltage up to 5 kV was applied to the PR sample, corresponding to an applied field of 50 V/μm. The signal beam is focused on the sample. Both the signal beam reflected from the sample surface and the reference beam are focused on the PR composite sample. The beams were p-polarized with equal intensities of 1 W/cm^2. The angle between the two beams and the tilted angle of the sample with respect to the normal vector were 30° and 60°, respectively. This leads to internal angles in the PR composites of 18.5° and 33.3°, respectively. The reference beam and the phase-modulated signal beam interfered inside the PR material. Due to the modulated refractive index in the PR composite sample, a grating is formed, the two beams are coupled, and the reference beam is diffracted in the direction of the speckled signal beam. The grating spacing with this tilted geometry is approximately 2.1 μm. Polarizing beam splitters and wave plates were used to adjust the ratio of the signal and reference beam intensities to their polarization inside the PR composite samples. After the PR composite, the beams were focused by means of a lens on a silicon photoreceiver (NewPort 1801-FS) with a bandwidth of 125 MHz.

Before carrying out LUS measurements, the coupling gains of the materials were determined. First, the signal beam with an intensity of $I_S = 1$ W/cm^2 was directed onto the PR sample and the transmitted intensity of the beam, I_S^t, after the PR composite was measured. Next, an electric field was applied to the PR sample, and the transmission intensity measurement of I_S^t was repeated. No changes in I_S^t and no fanning effect [7] in the PR sample were observed. Then, the reference beam of equal intensity $I_S = I_R$ was switched on and after several seconds switched off again. The transmitted intensities of both beams after the PR sample were monitored. The optical coupling gain was then calculated according to [9]:

$$\Gamma = \frac{1}{d}\left[\cos\theta_{1\,\mathrm{int}}\ln\left(\frac{I_S^t(I_R \neq 0)}{I_S^t(I_R = 0)}\right) - \cos\theta_{2\,\mathrm{int}}\ln\left(\frac{I_R^t(I_S \neq 0)}{I_R^t(I_S = 0)}\right)\right] \quad (1)$$

Here $\theta_{1\mathrm{int}}$, $\theta_{2\mathrm{int}}$ are the internal signal and reference beam angles, and d is the thickness of the PR sample.

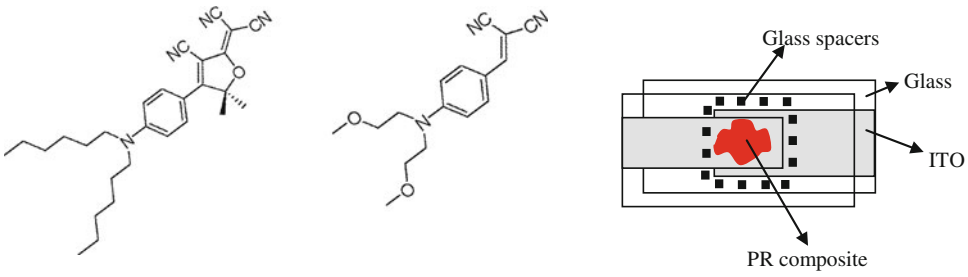

Fig. 1 Molecular structure of DCDHF-6 (**a**) and AODSCT (**b**). **c** Scheme of the photorefractive polymer composite beam combiner

(a) DCDHF-6 **(b)** AODCST **(c)** PR samples

The optical net coupling gains, $\Gamma_{\text{net}} = \Gamma - \alpha$, as a function of the external electric field follow a similar trend for both PR composites (Fig. 4). With increasing external voltage, the gain coefficients increase. The optical gain at 50 V/μm was calculated to be $\sim 60 \pm 2\ \text{cm}^{-1}$ for both composites. Breakdown usually limits applied field in PR polymer films. In our samples, breakdown was observed at voltages higher than 6–7 kV, corresponding to electric fields of 60 and 70 V/μm, respectively. Figure 4 indicates the necessity of a high electric field to achieve a high coupling gain. A good compromise between high coupling gain and safe operation to avoid electrical breakdown was found by carrying out experiments with voltages lower or equal to 5 kV.

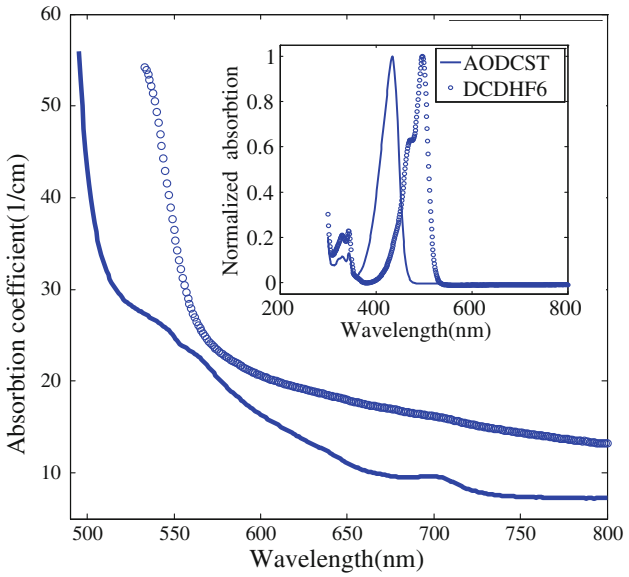

Fig. 2 Absorption coefficient of the polymer composites DCDHF-6:PVK:BBP:PCBM (*circles*) and AODCST:PVK:BBP:PCBM (*line*) between 500- and 800-nm wavelength. *Inset* normalized absorption of the composites in solution

The minimum detectable displacement, $\delta^{\min}$, on a sample surface is a crucial figure of merit for interferometers. It is defined as the sensitivity limit of an interferometer with a signal to noise ratio (SNR) of unity for 1-W signal beam power and 1-Hz electronic bandwidth. For an ultrasound detector based on a PR material, the SNR is given by [10]

$$\text{SNR} = 2(k_{\text{opt}})\delta\sqrt{\frac{\eta P}{h\nu B}}\, e^{\frac{-\alpha L}{2}} \frac{e^{\Gamma L} - 1}{\sqrt{e^{2\Gamma L} + 1}} \tag{2}$$

where $k_{\text{opt}} = 2\pi/\lambda_{\text{opt}}$, λ_{opt} is the optical wavelength, η is the quantum efficiency of the detector, P is the incidence power of beam on the detector, B is the electronic bandwidth, δ is the surface displacement, ν is the optical frequency, h is the Planck's constant, α is the absorption coefficient of the composite at λ, Γ is the optical two beam coupling gain of the PR composite, and L is the optical path length of the beams in the PR material. From Eqs. (1) and (2), the sensitivities of our LUS interferometers, $\delta^{\min}$, and the sensitivities at SNR = 1, 1 W and 1 Hz were determined. Incident optical signal beam powers of 171 and 185

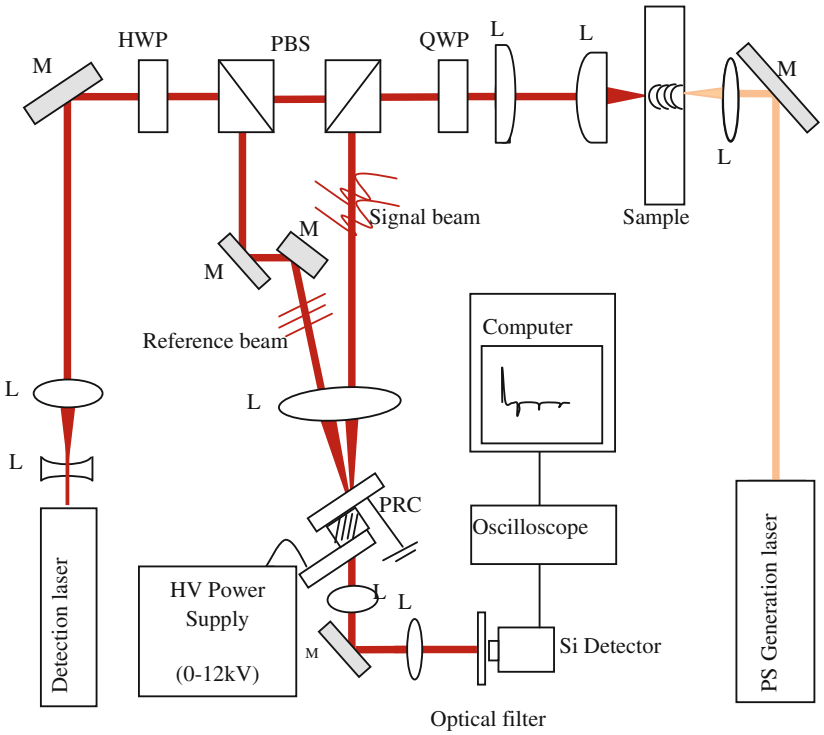

Fig. 3 Experimental setup of the polymer composites ultrasonic detector based on TWM measurements: *HWP* half-wave plate, *QWP* quarter wave plate, *PBS* polarizer beam splitter, *M* mirror, *L* lens, *PRC* photorefractive polymer composites

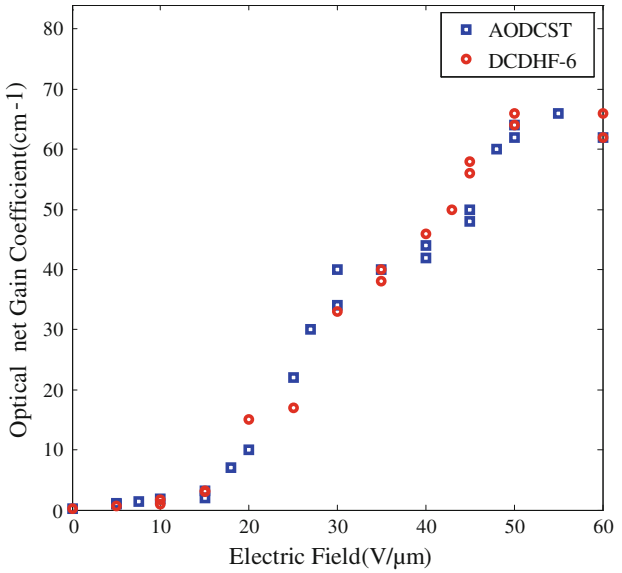

Fig. 4 Optical net gain coefficient versus applied electric field for AODCST/PVK/C60/BBP (*squares*) and DCDHF-6/PVK/C60/BBP (*circles*)

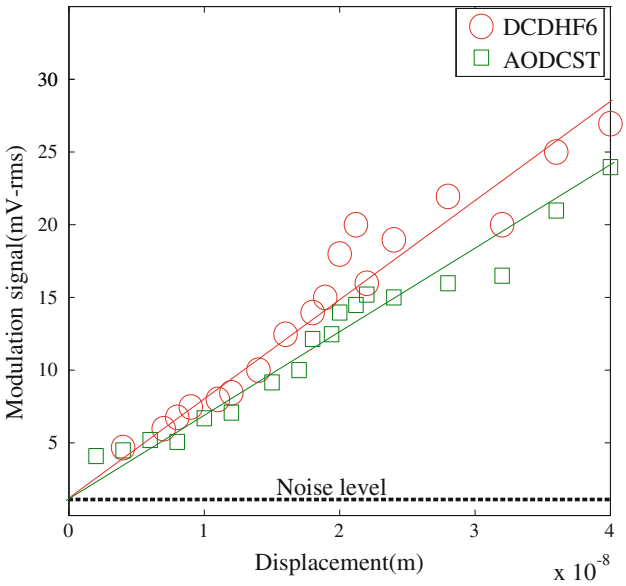

Fig. 5 Amplitude of the modulated signals received by PR detectors based on DCDHF-6 and AODCST as a function of the applied ultrasonic amplitude at 100 Hz

μW were measured on a 125-MHz photoreceiver with $\eta = 0.63$ for both PR composites at 50-V/μm electric field. The sensitivity of both LUS interferometers was calculated to be $\sim$0.1 nm, which corresponds to a sensitivity limit of $\sim$9.5 10^{-8} nm $(W/Hz)^{0.5}$.

To measure the sensitivities of the PR polymer detectors, a transducer with resonance frequency of 500 kHz and maximum stroke of 3 μm/150 V was used. As a sample, a small circular mirror with 4 mm diameter was mounted on the transducer surface to reflect the phase-modulated signal beam. Firstly, a Michelson interferometer was used to calibrate and investigate the linear response of the transducer for different applied voltage. By applying sinusoidal signals with different amplitudes to the transducer, the linear response of the transducer for applied voltages from 0.05 to 150 V was found and then the calibrated transducer was used in each PR polymer setup to detect the ultrasonic displacements.

We observed that the frequency response of our PR polymers for the frequencies above 10 Hz is constant, and therefore, to characterize the PR interferometers, the transducer was driven at a frequency of 100 Hz by applying low voltages. The generated sinusoidal displacements were detected by using the LUS receivers, and Fig. 5 shows the amplitudes of the detected signals as a function of the applied vibration amplitudes of the mirror. The signals amplitude increases linearly with the applied vibration amplitude for both polymers.

Minimum detectable displacement (sensitivity) can be measured by using the noise level line, which is a main limiting parameter in a PR interferometer. For a detector, at very low laser power, the noise level is very low about zero (low-amplitude electronic noise and no photonic noise), but in our experiments, the input laser power to the photodetector after the polymer samples is more than 170 μW, which increases the photonic noise in the photodetector. The other noise that contributes to the experiment results is the electronic noise. These two noises will increase the total noise level ($\sim$1 mV in the experiments) and can limit the interferometer sensitivity. The smallest measurable displacement for our PR composites was estimated around 0.2 nm, which agrees well with the calculated value of 0.1 nm.

In order to estimate the speed of the LUS interferometers, the response times, τ, of the PR materials have to be determined [2, 10]. The hologram formation time is given by the separation, transportation and trapping time of the electrons and holes over the grating space, which causes the generation of an internal space charge electric field and an index grating in the PR material. One method to measure the speed of the PR composites is to modulate the single beam phase at different frequencies [2]. Figure 6 displays the amplitudes of the detected signal beams as a function of the applied frequency on the transducer for the PR composites based on DCDHF-6 and AODCST. Both PR composites show a similar frequency response, but with different response times. To evaluate the response times of the organic PR composites, theoretical curves given by [2]

$$A(f) = A_0 \left[\frac{2\pi f \tau}{(1 + (2\pi f \tau)^2)^{1/2}} \right] \quad (3)$$

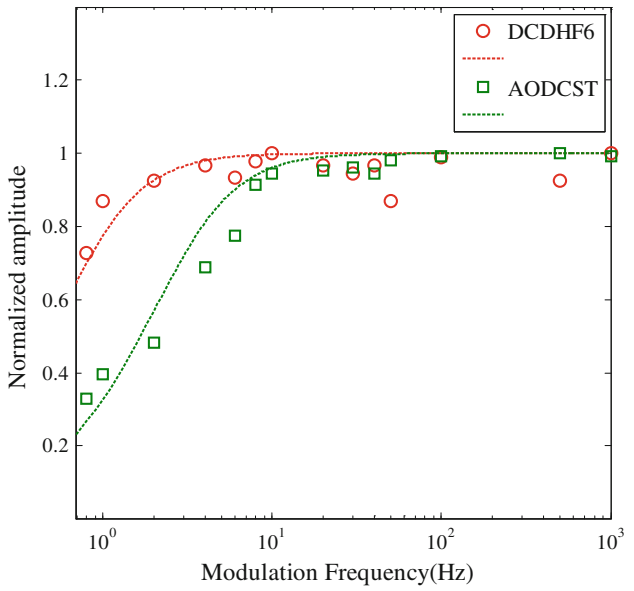

Fig. 6 Modulated amplitudes as a function of frequency for LUS detector based on DCDHF-6 (*circles*) and AODCST (*squares*) PR polymer composites. The *dashed lines* display fits to the experimental data

were fitted to the data points. Here A_0 is the modulation amplitude, f is the modulation frequency, and τ is the response time of PR material. The grating formation times from curve fitting (dashed lines in Fig. 6) for the DCDHF-6 and AODCST composites were determined to be approximately 195 and 60 ms, respectively, which correspond to cutoff frequencies ($f_{\text{cut}} = 1/2\pi\tau$) of $\sim$1 and 3 Hz. Note that these results were measured under the same experimental conditions. The grating response times could be made faster by applying higher electric fields to the samples or by using higher laser intensities of the interfering beams inside the PR composites [2].

2.3 LUS measurements

The previous experiments suggest the important application of our polymer-based LUS receiver for the contactless measurement of metal sheet thicknesses, for example, in steel industry [1]. For samples with scattering surfaces, an interferometer based on a PR material is particularly suited, as the reference beam is adapted to the scattered signal beam. Thus, such an interferometer allows, for example, online investigation of hot moving metal plates to determine the thickness and detect the defects such as holes and surface cracks where contacting methods are prohibited. Such measurements can be performed by investigation of reflected surface and bulk waves in material and their time of flight.

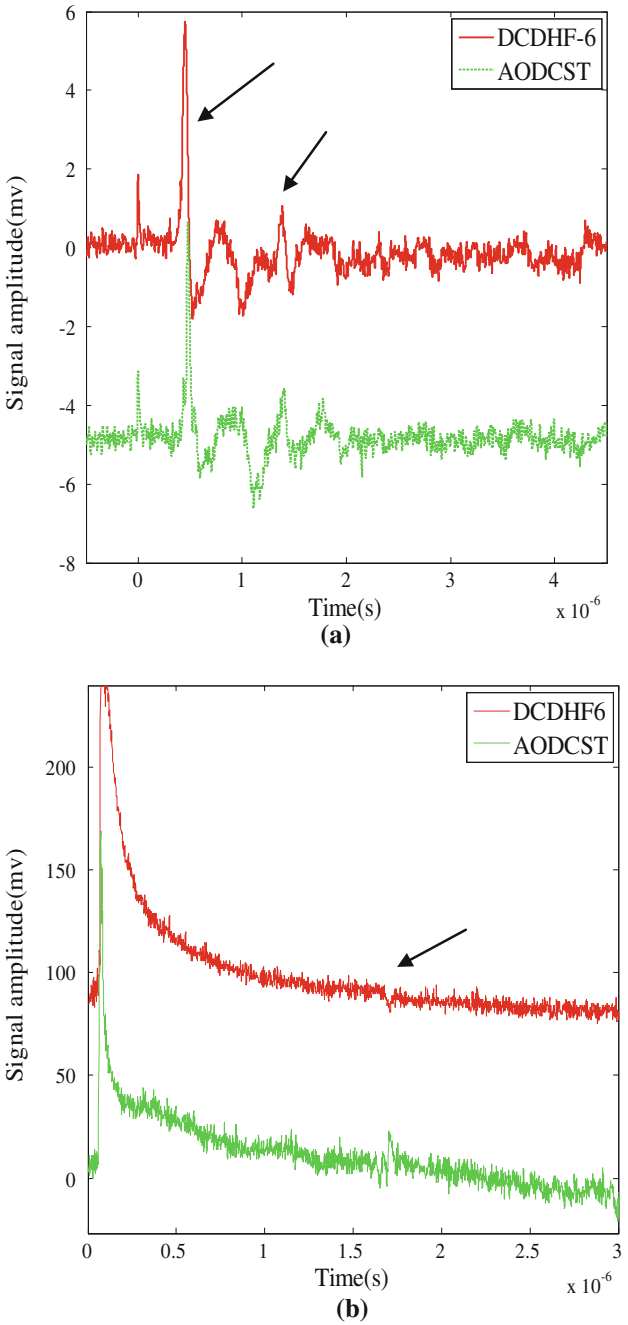

Fig. 7 Measured longitudinal echoes detected in transmission geometry on (**a**) an aluminum sheet with 3 mm thickness (**b**) on a 9-mm-thick steel sample using DCDHF-6:PVK:BBP:PCBM (*red lines*) and AODCST:PVK:BBP:PCBM (*green lines*) photorefractive polymer interferometers at 50 V/μm

2.3.1 *Contactless thickness measurement*

To demonstrate the suitability of our LUS receivers for the remote thickness measurement of metal sheets, experiments were carried out on a 3-mm-thick aluminum sheet and a 9-mm-thick steel plate. To investigate the aluminum and steel plate thicknesses, pulses from a 1,064-nm

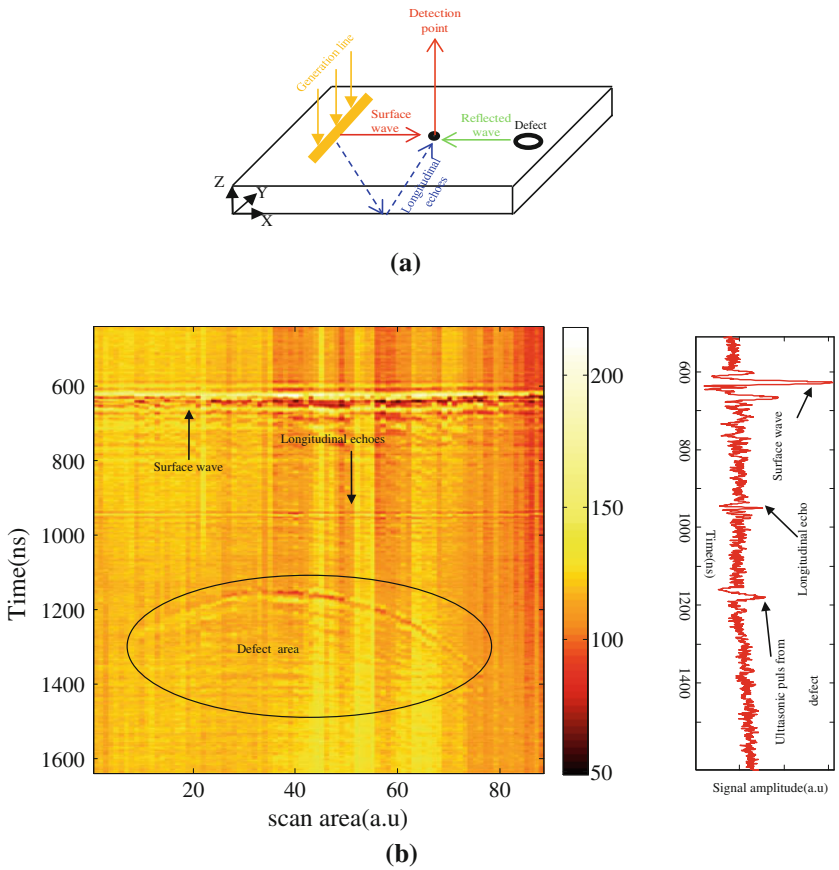

Fig. 8 **a** Schematic of the experimental arrangement for defect detection on the surface of a 3-mm-thick aluminum sheet based on an AODCST:PVK:BBP:PCBM photorefractive interferometer using a line generation with 5 mJ energy (**b**). Detected ultrasonic signals of the surface (Rayleigh), longitudinal bulk waves and reflected surface waves from the surface defect, clearly display the defect profile

Nd:YAG laser were focused on the backside of the samples with pulse lengths of 20 ps, an energy of 5 mJ and a spot size of 50 μm to generate ultrasonic displacements (Fig. 3). The reflected longitudinal waves on the front side of the sample were detected utilizing both LUS PR polymer composites. The resulting time traces were acquired using a digital oscilloscope. For all experiments, the reference and the signal beam intensities on the samples were equal (1 W/cm^2); the applied voltage was 5 kV.

Figure 7 shows that under similar experimental conditions, the detected bulk ultrasonic echoes on the surface of the 3-mm-thick aluminum sample (a) and on the 9-mm-thick steel sample (b) are clearly distinguishable. At time $t = 0$, a positive pulse can be identified, which is the result of coupling of the picosecond excitation pulse into the detection system. By using an infrared optical filter in front of the photodiode, this pulse could be reduced. For the aluminum sample, the detected ultrasonic echoes are periodic.

We measured the upper limitation frequency of the setup by calculation frequency spectrum of the first longitudinal pulses which changes from 25 to 30 MHz. It is strongly depended to the excitation laser spot size on the sample surface. The compensation frequency (cutoff frequency) is lower than 10 Hz, and above this frequency, the setup has a flat frequency response (Fig. 6).

By using the period of the displacement signals of ~940 ns and the longitudinal ultrasound velocity of approx. 6,400 m/s for aluminum, a thickness of 3.08 mm was determined. For the steel sample, only one pulse could be detected. The time of flight of the first echo was measured to be ~1,570 ns. This results in a sample thickness of 8.9 mm.

2.3.2 *Remote defect detection*

Industrial applications of noncontact ultrasound interferometers are found in the detection of surface defects. The technique allows for the estimation of the defect position and profile with good spatial resolution [1]. We have prepared a sample with an artificial hole of 1 mm radius as surface flaw on a 3.5-mm-thick aluminum plate, to demonstrate the capability of our fast AODCST:PVK:BBP:PCBM LUS detectors. As shown in Fig. 8a, we have scanned the sample surface with a laser line of 8 mm length, 100 μm width and 5 mJ energy. To keep the distance constant between the generated laser line on the sample and the detection point, the sample was moved in *Y* direction about 6.5 mm with a scan step of 75 μm.

Figure 8b shows the detected ultrasonic signals of the surface (Rayleigh), longitudinal bulk waves and the

reflected surface waves from the surface defect which obviously displays the defect profile. From the surface and longitudinal wave speeds, about 3,000 and 6,400 m/s in aluminum, the defect location, the defect profile and the sample thickness are accurately determined.

3 Conclusions

In conclusion, we used two PR polymer composites, DCDHF-6:PVK:BBP:PCBM and AODCST:PVK:BBP:PCBM, as photorefractive materials in a homodyne LUS interferometer. We showed that the ultrasonic detector based on the AODCST as nonlinear optical chromophore has a faster response time ($\sim$60 ms) than that with DCDHF-6. For detection of ultrasound waves, both LUS polymer detectors showed the same sensitivity ($\sim$0.1 nm). The polymer ultrasound receivers were successfully used to detect ultrasonic displacements on a 3-mm-thick aluminum plate and a 9-mm-thick steel sample. By measuring the time of flight of the detected longitudinal bulk waves in the samples, thicknesses of 3.08 and 8.9 mm were calculated for aluminum and steel plates, respectively. The fast ultrasonic AODCST:PVK:BBP:PCBM detector was successfully used to detect a surface defect. The profile and the location of a hole with 1 mm radius on the surface of an aluminum sample were accurately determined. The LUS measurements show the large potential of organic polymer-based ultrasonic receivers for noncontact and nondestructive testing investigations on metal sheets.

Acknowledgments This work has been supported by the Christian Doppler Research Association, the K-Project for Non-Destructive Testing and Tomography supported by the COMET-Program of the Austrian Research Promotion Agency (FFG), Grant No. 820492, the European Regional Development Fund (EFRE) in the framework of the EU-program Regio 13 and the federal state of Upper Austria. We are also indebted to Spanish MINECO and Comunidad Valenciana for funding (projects CTQ2010-20349 and PROMETEO/2012/010).

References

1. C.B. Scruby, L.E. Drain, *Laser Ultrasonics: Techniques and Applications* (Adam Hilger, Bristol, 1990)
2. T. Honda, T. Yamashita, H. Matsumoto, Jpn. J. Appl. Phys. **34**, 3737 (1995)
3. B.F. Pouet, R.K. Ing, S. Krishnaswamy, D. Royer, Appl. Phys. Lett. **69**, 3782–3784 (1996)
4. O. Ostroverkhova, W.E. Moerner, Chem. Rev. **104**, 3267–3314 (2004)
5. F.G. Gómez, J.C. Álvarez-Santos, J.L. Rodríguez- Redondo, E. Font-Sanchis, J.M. Villalvilla, Á. Sastre-Santos, M.A. Díaz-García, F. Fernández-Lázaro, J. Mater. Chem. **22**, 12220–12228 (2012)
6. M.B. Klein, G.D. Bacher, A. Grunnet-Jepsen, D. Wright, W.E. Moerner, Opt. Commun. **162**, 79–84 (1999)
7. U. Gubler, M. He, D. Wright, Y. Roh, R. Twieg, W.E. Moerner, Adv. Mater. **14**, 313–317 (2002)
8. M.A. Díaz-García, D. Wright, J.D. Casperson, B. Smith, E. Glazer, W.E. Moerner, Chem. Mater. **11**, 1784–1791 (1999)
9. J.L. Maldonado, Y. Ponce-de-León, G. Ramos-Ortíz, M. Rodríguez, M.A. Meneses-Nava, O. Barbosa-García, R. Santillán, N. Farfán, J. Phys. D Appl. Phys. **42**, 075102 (2009)
10. T. Kundu, *Ultrasonic Nondestructive Evaluation: Engineering and Biological Material Characterization* (CRC Press LLC, Boca Raton, 2004)